Basic Properties of Slow-Fast Nonlinear Dynamical System in the Atmosphere-Ocean Aggregate Modeling

SERGEI SOLDATENKO[1] and DENIS CHICHKINE[2]
[1]Center for Australian Weather and Climate Research
Earth System Modeling Research Program
700 Collins Street, Melbourne, VIC 3008
AUSTRALIA
s.soldatenko@bom.gov.au
[2]University of Waterloo
Faculty of Mathematics
200 University Avenue West, ON N2L 3G1
CANADA

Abstract: Complex dynamical processes occurring in the earth's climate system are strongly nonlinear and exhibit wave-like oscillations within broad time-space spectrum. One way to imitate essential features of such processes is using a coupled nonlinear dynamical system, obtained by combining two versions of the well-known Lorenz (1963) model with distinct time scales that differ by a certain time-scale factor. This dynamical system is frequently applied for studying various aspects of atmospheric and climate dynamics, as well as for estimating the effectiveness of numerical algorithms and techniques used in numerical weather prediction, data assimilation and climate simulation. This paper examines basic dynamic, correlation and spectral properties of this system, and quantifies the influence of the coupling strength on power spectrum densities, spectrograms and autocorrelation functions.

Key-Words: dynamical system, earth's climate system, numerical weather prediction, spectral properties

1 Introduction

Theory of dynamical systems enables us to explore temporal and spatial evolution of the earth's climate system and its components [1]. The "earth's climate system" is a term that is used to refer to the interacting atmosphere, hydrosphere, lithosphere, cryosphere, biosphere as well as numerous natural and anthropogenic physical, chemical, and biological cycles of our planet. Each of these components has unique dynamics and physics, and is characterised by specific time-space spectrum of motions, characteristic time, internal variability, and other properties [2].

Dynamical processes occurring in the earth's climate system have turbulent nature and exhibit wave-like oscillations within broad time-space spectrum, and, therefore, are characterized by strong nonlinearity [3]. In this context, numerical weather prediction (NWP) and climate simulation represent one of the most complex and important applications of dynamical systems theory and its concepts and methods.

It is important to emphasize, that NWP and climate simulation focus on processes with very different time scales and, in more importantly, pursue very different objectives [4, 5]. NWP is a typical initial value problem aiming to predict, as precisely as possible, the future state of the atmosphere taking into account current (initial) weather conditions. To date, due to the intrinsic limits with regards to the predictability of atmospheric processes, the practical importance of NWP is limited to a time horizon of 7 – 10 days. Errors in the NWP are primarily generated by inaccuracies in the initial conditions rather than by the imperfections in mathematical models [6]. By contrast, climate change and variability simulations focus on much longer time scales (several months or even years) and involve the study of stability of climate model attractors with respect to external forcing. Despite these fundamental differences, deterministic mathematical models, based on the same physical principles and fundamental laws of physics such as conservation of momentum, energy and mass, are commonly applied to both NWP and climate simulations. Mathematically, these physical laws and principles are generally expressed in terms of a set of nonlinear partial differential equations (PDEs) and, in their discrete form, contain a large number of state variables and parameters.

Performing a detailed simulation of the dynamics of the earth's climate system and its components using such models requires significant computational resources and considerable time for analysis and interpretation of obtained results. Consequently, low-order models have drawn attention of scientists as very compact and convenient tools for studying various aspects of dynamics of natural physical processes and phenomena, and also for estimating the effectiveness of numerical algorithms and techniques used in computational simulations.

To simulate and predict the behavior and changes in the earth's climate system, integrated models that link together models of the atmosphere, oceans, sea-ice, land surface, biochemical cycles including those of carbon and nitrogen, chemistry and aerosols are required. In environmental, geophysical and engineering sciences one of the most widely used low-order systems is a coupled system obtained by combining of several versions of the well-known original Lorenz system [7] (hereinafter referred to as the L63 system) with distinct time scales differing by a certain time-scale factor. Coupling of two systems, one with "fast" and another with "slow" time scales, allows imitating the interaction between a fast-oscillating atmosphere and slow-fluctuating ocean. This coupled system was successfully applied to climate studies (e.g. [8, 9]), numerical weather prediction and data assimilation (e.g. [10-12]), sensitivity analysis, parameter estimations and predictability studies (e.g. [13 – 16]). The coupled Lorenz system, in spite of its simplicity, is capable of simulating some essential properties of the general circulation of the atmosphere and ocean and allows, with negligible computational costs, to obtain realistic and reasonable qualitative and quantitative results, while retaining the essential physics. The correct application of this system requires knowledge of its dynamics, spectral and other properties.

This paper will look at the basic properties of a coupled chaotic nonlinear system obtained by combining "fast" and "slow" versions of the L63 system, corresponding to time scales of the NWP and climate variability simulations respectively.

2 Coupled Dynamical System

2.1 Dynamical system concept

In the most general sense, an abstract dynamical system can be formally specified by its state vector the coordinates of which (state or dynamic variables) characterize exactly the state of a system at any moment, and a well-defined function (i.e. rule) which describes, given the current state, the evolution with time of state variables. There are two kinds of dynamical system: continuous time and discrete time. Continuous-time dynamical systems are commonly specified by a set of ordinary or partial differential equations and the problem of the evolution of state variables in time is then considered as an initial value problem. With respect to the earth system simulations, discrete-time deterministic systems are of particular interest, because, in a general case, the solution of differential equations describing the evolution of the earth's climate system and its subsystems can be only obtained numerically.

Let the current state of an abstract dynamical system is defined by the following set of n real variables $u_1, u_2,\ldots,u_n$. The number n is referred as the dimension of the system. A particular state $u = (u_1, u_2,\ldots,u_n)$ corresponds to a point in an n-dimensional space $U\subseteq\mathbb{R}^n$, the so-called phase space of the system. Let $t_m\in\mathbb{Z}$ $(m=0,1,2,\ldots)$ be the discrete time, and $f = (f_1, f_2,\ldots,f_n)$ is a smooth vector-valued function defined in the domain $U\subseteq\mathbb{R}^n$. The function f describes the evolution of the system state from the moment of time t_0=0 to the state of the system at the moment of time t_m such that f: $U\rightarrow U$. Thus, a deterministic dynamical system with discrete time can be specified by the following equations:

$$u\left(t_{m+1}\right)=f\left(u\left(t_m\right)\right),\ u\left(t_0\right)=u_0, \qquad (1)$$
$$m=0, 1, 2, \ldots .$$

The sequence $\left\{u\left(t_m\right)\right\}_{m=0}^{\infty}$ is a trajectory of the system (1) in its phase space $u\in U$, which is uniquely defined by the initial values of state variables u_0 (initial conditions):

$$u\left(t_m\right)=f^m\left(u_0\right), \qquad (2)$$

where $f^m\left(u_0\right)$ denotes a m-fold application of f to u_0.

In relation to modeling of the earth's climate system, the vector-function f is a nonlinear function of the state variables. Nonlinearity can arise from the numerous feedbacks existed between the different components of the system, external forcing caused by natural and anthropogenic processes and the chaotic nature of dynamical processes occurring in geospheres.

2.2 Coupled nonlinear dynamical system

A multiscale nonlinear dynamical system examined in this paper is derived by coupling the fast and slow versions of the original L63 system [7] and can be written as follows [17, 18]:

a) the fast subsystem

$$\dot{x} = \sigma(y - x) - c(aX + k),$$

$$\dot{y} = rx - y - xz + c(aY + k),$$

$$\dot{z} = xy - bz + c_z Z,$$

b) the slow subsystem

$$\dot{X} = \varepsilon\sigma(Y - X) - c(x + k),$$

$$\dot{Y} = \varepsilon(rX - Y - aXZ) + c(y + k),$$

$$\dot{Z} = \varepsilon(aXY - bZ) - c_z z,$$

where lower case letters x, y and z represent the dynamic variables of the fast model, capital letters X, Y and Z denote the state variables of the slow model, $\sigma>0$, $r>0$ and $b>0$ are the parameters of the original L63 model, ε is a time-scale factor (if, for instance, ε =0.1 then the slow subsystem is ten times slower than the fast subsystem), c is a coupling strength for x, X, y and Y variables, c_z is a coupling strength parameter for z and Z variables, k is a "decentring" parameter [17], and a is a parameter representing the amplitude scale factor (for instance, a=1 indicates that slow and fast subsystems have the same amplitude scale). The coupling strength parameters c and c_z control the interconnection between fast and slow subsystems: the smaller the parameters c and c_z, the weaker the interdependence between two subsystems. Without loss of generality, one can assume that a=1, k=0 and c=c_z, then equations of the model can be represented in an operator form as follows

$$\frac{du}{dt} = A(u;\, p)u\,, \tag{3}$$

where $u=(x,y,z,X,Y,Z)^{\mathrm{T}}$ is a model state vector, $p=(\sigma,b,r,\varepsilon,c)^{\mathrm{T}}$ is a vector of model parameters, and $A(u; p)$ is the matrix operator such that

$$A = \begin{bmatrix} -\sigma & \sigma & 0 & -c & 0 & 0 \\ r & -1 & -x & 0 & c & 0 \\ 0 & x & -b & 0 & 0 & c \\ -c & 0 & 0 & -\varepsilon\sigma & \varepsilon\sigma & 0 \\ 0 & c & 0 & \varepsilon r & -\varepsilon & -\varepsilon X \\ 0 & 0 & -c & 0 & \varepsilon Y & -\varepsilon b \end{bmatrix}$$

Thus, system of autonomous ODEs (3) has five control parameters (σ, r, b, c and ε) and together with given initial conditions $u(t_0)=u_0$ represents an initial value problem.

2.3 Equations in variational form

Equations in variational form are used to study the system's dynamical properties. These equations can be obtained by linearization of (3) around a certain trajectory, which is a particular solution of (3) and represents a vector-function $u(t)$, $t\in[0,\infty)$. Assume that the system (6) operates along the trajectory $u^*(t)$ and let $\delta u(t)$ be an infinitesimal perturbation of the state vector, i.e. $\delta u(t) = u(t) - u^*(t)$. Approximating the right-hand side of (6) by a Taylor expansion in the vicinity of $u^*(t)$ and neglecting 2nd order and higher order terms, one can obtain the following set of linear ODEs, the equations in variations:

$$\frac{d\delta u(t)}{dt} = J\delta u(t), \qquad \delta u(t_0) = \delta u_0\,, \tag{4}$$

where $J = \left.\dfrac{\partial A}{\partial u}\right|_{u=u^*}$ is a Jacobean matrix:

$$J = \begin{bmatrix} -\sigma & \sigma & 0 & -c & 0 & 0 \\ (r - z) & -1 & -x & 0 & c & 0 \\ y & x & -b & 0 & 0 & c \\ -c & 0 & 0 & -\varepsilon\sigma & \varepsilon\sigma & 0 \\ 0 & c & 0 & \varepsilon(r - Z) & -\varepsilon & -\varepsilon X \\ 0 & 0 & -c & \varepsilon Y & \varepsilon X & -\varepsilon b \end{bmatrix}$$

Variational equations (4) can be rewritten as

$$\delta u(t) = L_t \delta u_0, \qquad \delta u(t_0) = \delta u_0\,, \tag{5}$$

where L_t is a linear solution operator.

2.4 Model parameters

The time evolution of coupled nonlinear system (3) is conditioned by a set of ODEs and control parameters σ, r, b, c and ε. By setting parameter c equal to zero, one can restore the original L63 model. Standard values of the L63 parameters corresponding to chaotic behaviour are: $\sigma = 10,\ b = 8/3,$ and $r = 28$ [7]. These parameters are used in this study since the motions in the atmosphere and ocean are inherently chaotic. It is important to note, that for $\sigma = 10$ and $b = 8/3$ there is a critical value for parameter r, equal to 24.74, and any r larger than 24.74 induces chaotic behaviour of the L63 system [19]. The time scale factor ε is taken to be 0.1. Thus, in our study, the main control parameter is the coupling strength c, which essentially determines the strength of

interactions between fast and slow models and, therefore, the behaviour of the entire coupled system. In numerical experiments values of this parameter have been chosen in accordance with [17, 18]: $c \in [0.15,\ 1.0]$.

2.5 Numerical integration procedure

The system of equations (3) is numerically integrated by applying a fourth order Runge-Kutta algorithm with a time step $\Delta t = 0.01$. To begin with, equations (3) are transformed into a discrete-time form and then integrated. This integration produces time-series for each of the dynamic variables at equally-spaced time-points starting from t_0, denoted by

$$\{u_m = u(t_m),\ t_m = m\Delta t,\ m = 0,\ldots,M-1\},$$

where Δt is the integration time step, also known as the sampling interval. To discard the initial transient period the numerical integration starts at time $t_{-T} = -2^{14}\Delta t$ with the initial conditions

$$u_{-T} = (0.01;\ 0.01;\ 0.01;\ 0.02;\ 0.02;\ 0.02)^{\mathrm{T}} \quad (6)$$

and finishes at time t_0. In addition, this ensures that the calculated vector of dynamic variables u_0=$u(t_0)$ is on the system's attractor. The state vector u_0 is then used as the initial conditions for further numerical experiments. Note that, for $\Delta t = 0.01$, the numerical integration with length of 100 time steps corresponds to one non-dimensional unit of time.

3 Coupled System Properties

3.1 Equilibrium points

Equilibrium (fixed) points of the system of ODEs (3) occur whenever $\dot{u} = 0$. Because this system is homogeneous, it has at least a trivial solution, which is also one of the equilibrium points. In addition, for given parameter values, system (3) has eight non-trivial equilibrium points, all of which can be found numerically. Coordinates of fixed points depend on the parameter *c* and are listed in Table 1 for *c* = (0.8; 0.15). The stability of the system in the local vicinity of equilibrium points can be studied by evaluating the Jacobean matrix *J* at each of the fixed points of the system (3) and then finding the resulting eigenvalues. If at least one eigenvalue has a positive real part, the equilibrium is an unstable node. For instance, for *c*=1.0 at the origin, the Jacobean has the following six eigenvalues

$$\lambda_1 = -22.87,\ \lambda_2 = 11.90,\ \lambda_3 = 1.22,$$
$$\lambda_4 = -2.35,\quad \lambda_5 = -2.13,\ \lambda_6 = -0.80.$$

Since two of the eigenvalues are positive, the origin is an unstable node and since the remaining four of the eigenvalues are negative this point is saddle. Stability of the system in the vicinity of the remaining fixed points can be examined analogously.

Table 1: Non-trivial equilibrium points of the coupled system for *c*=0.15 (numerator) and *c*=0.8 (denominator)

x_0	y_0	z_0	X_0	Y_0	Z_0
8.6244 / 11.9392	8.6202 / 11.8783	27.0182 / 27.5491	–0.2751 / –0.7612	1.0186 / 8.7902	–15.3028 / –85.2914
–8.6244 / –11.9392	–8.6202 / –11.8783	27.0182 / 27.5491	0.2751 / 0.7612	–1.0186 / –8.7902	–15.3028 / –85.2914
8.3103 / 7.8413	8.1437 / 6.2459	26.8420 / 25.8088	–11.1123 / –19.9433	–9.8657 / –13.6702	26.0129 / 24.8091
–8.3103 / –7.8413	–8.1437 / –6.2459	26.8420 / 25.8088	11.1123 / 19.9433	9.8657 / 13.6702	26.0129 / 24.8091
8.1879 / 6.7233	8.3404 / 7.9473	27.1900 / 29.2784	10.1619 / 15.2997	11.3901 / 20.6783	28.1103 / 30.8040
–8.1879 / –6.7233	–8.3404 / –7.9473	27.1900 / 29.2784	–10.1619 / –15.2997	–11.3901 / –20.6783	28.1103 / 30.8040
0.0457 / 0.4400	–0.0837 / –0.5140	1.5182 / 8.1275	–8.6242 / –11.9254	–8.6174 / –11.5734	27.3743 / 27.0154
–0.0457 / –0.4400	0.0837 / 0.5140	1.5182 / 8.1275	8.6242 / 11.9254	8.6174 / 11.5734	27.3743 / 27.0154

3.2 Dissipativity

Let V be the volume of some region of phase space. The rate of volume contraction is given by Lie derivative,

$$\frac{1}{V}\frac{dV}{dt}=\frac{\partial\dot{x}}{\partial x}+\frac{\partial\dot{y}}{\partial y}+\frac{\partial\dot{z}}{\partial z}+\frac{\partial\dot{X}}{\partial X}+\frac{\partial\dot{Y}}{\partial Y}+\frac{\partial\dot{Z}}{\partial Z}=$$
$$-(1+\varepsilon)(1+\sigma+b)=\alpha<0.$$

Since the rate of volume contraction is always negative under the chosen model parameters, the coupled system (3) is dissipative and, therefore, volumes in phase space shrink exponentially with time. This is represented mathematically by

$$V(t)=V(t_0)e^{\alpha t}.$$

3.3 Symmetry and invariance

One can easily to show that the coupled system (3) remains invariant under the transformation

$$F:\ (x,y,z,X,Y,Z)\to(-x,-y,z,-X,-Y,Z).$$

This means that if

$$\big(x(t),y(t),z(t),X(t),Y(t),Z(t)\big)$$

is a solution of (3), then

$$\big(-x(t),-y(t),z(t),-X(t),-Y(t),Z(t)\big)$$

is also a solution. The invariance of z and Z axes indicates that all trajectories on the z and Z axes remain on these axes and approach the origin. Indeed, if

$$(x_0,y_0,z_0,X_0,Y_0,Z_0)=(0,0,z_0,0,0,Z_0),$$

then the model equations are as follows

$$\dot{z}=-bz+cZ\,, \tag{7}$$

$$\dot{Z}=-\varepsilon bZ-cz\,. \tag{8}$$

Differentiating equation (7) with respect to t and then substituting equation (8) into the result of differentiation gives the following second order ODE

$$\ddot{z}+b(1+\varepsilon)\dot{z}+\left(c^2+\varepsilon b^2\right)z=0\,.$$

This equation is a dumped harmonic oscillator which can be rewritten as

$$\ddot{z}+2\gamma\dot{z}+\omega_0^2 z=0\,, \tag{9}$$

where $\gamma=b(1+\varepsilon)/2$ is a damping constant, and $\omega_0^2=\left(c^2+\varepsilon b^2\right)$ is a natural frequency.

Equation (9) is a linear homogeneous ODE and its general solution depends on the relationship between damping constant γ and natural frequency ω_0.

In our example a damping constant $\gamma\approx 1.47$ and the natural frequency ω_0 depends on the coupling strength parameter c (Table 2). Critical frequency ω_0^c, at which $\gamma=\omega_0$, occurs when $c\approx 1.2$. Since for our experiments $c\in[0.15;\ 1.0]$, oscillator (10) is over-dumped ($\gamma>\omega_0$) and its general solution is given by the following equation

$$z(t)=Ae^{-\beta_1 t}+Be^{-\beta_2 t}, \tag{10}$$

where $\beta_{1,2}=\gamma\pm\omega_0\sqrt{(\gamma/\omega_0)^2-1}$, and A, B are unknown constants of integration. The solution of equation (10) asymptotically tends to the equilibrium z=Z=0 without oscillations: as $t\to\infty$, the dynamic variables z and Z tend to zero.

Table 2: Natural frequency ω_0 for different values of the coupling strength parameter

c	0.01	0.15	0.5	0.8	1.0	1.2	1.5
ω_0	0.8422	0.8565	0.9804	1.1624	1.3081	1.4667	1.7208

3.4 System attractor

The structure of the resulting attractor depends on the coupling strength parameter c. Figs. 1 and 2 illustrate phase portraits in x–y, x–z, and y–z phase planes of both fast and slow subsystems for weak (c=0.15) and strong (c=0.8) coupling, respectively.

It is known, that the L63 model produces chaotic oscillations of a switching type: the structure of its attractor contains two regions divided by the stabile manifold of a saddle point in the origin. For relatively small coupling strength parameter (c<0.5), the attractor for both fast and slow subsystems maintains a chaotic structure, which is inherent in the original L63 attractor. As the parameter c increases, the attractor for both fast and slow subsystems undergoes structural changes breaking the patterns of the original L63 attractor.

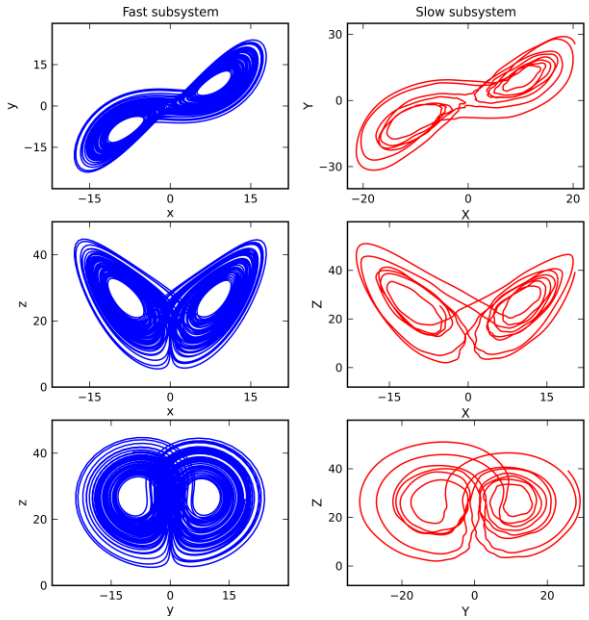

Fig. 1: Phase portraits for fast and slow subsystem for c=0.15.

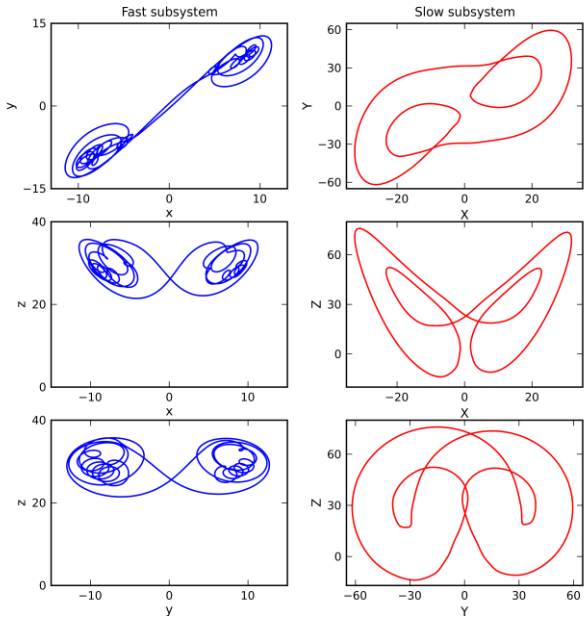

Fig. 2: Phase portraits for fast and slow subsystem for c=0.8.

Fast and slow subsystems affect each other through coupling terms, and at some value of the coupling strength parameter ($c > 0.5$) a chaotic behavior is destroyed and dynamic variables begin to exhibit some sophisticated motions which are not obviously periodic. Moreover, qualitative examination shows that the evolution through time of both subsystems becomes, to large degree, synchronous (however, phase synchronization requires specific analysis which is not within the scope of this paper). For example, for c=0.8 the plane phase portraits $X - Y$, $X - Z$ and $Y - Z$ of the slow subsystem represent closed curves which are mostly smooth and have no visible kinks. These portraits indicate that the motion possesses periodic properties. At the same time, the attractor of the slow subsystem for c=0.8 has a more complex structure.

3.4 Correlation properties

Numerical integration of equations (3) produces the time series of dynamic variables hereinafter referred to as signals or oscillations. We can conduct the diagnosis of the coupled dynamical system by analysing the signals using standard tools such as autocorrelation functions and the distribution of power density in the frequency domain from signals obtained in the time domain.

Autocorrelation functions (ACFs) enable one to distinguish between regular and chaotic processes and to detect transition from order to chaos. In particular, for chaotic motions, ACF decreases in time, in many cases exponentially, while for regular motions, ACF is unchanged or oscillating. In general, however, the behaviour of ACFs of chaotic oscillations is frequently very complicated and depends on many factors (e.g. [20, 21]). Autocorrelation functions can also be used to define the so-called typical time memory (typical timescale) of a process [22]. If it is positive, ACF is considered to have some degree of persistence: a tendency for a system to remain in the same state from one moment in time to the next. The ACF for a given discrete dynamic variable $\{u_m\}_{m=0}^{M-1}$ is defined as

$$C(s) = \langle u_m u_{m+s} \rangle - \langle u_m \rangle \langle u_{m+s} \rangle,$$

where the angular brackets denote ensemble averaging. Assuming time series originates from a stationary and ergodic process, ensemble averaging can be replaced by time averaging over a single normal realization

$$C(s) = \langle u_m u_{m+s} \rangle - \langle u \rangle^2.$$

Signal analysis commonly uses the normalized ACF, defined as $R(s) = C(s)/C(0)$.

ACF plots for realizations of dynamic variables x and X, and z and Z calculated for different values of the coupling strength parameter c are presented in Figs. 3 and 4, respectively. For relatively small parameter c ($c < 0.4$), the ACFs for both x and X variables decrease fairly rapidly to zero, consistently with the chaotic behaviour of the coupled system.

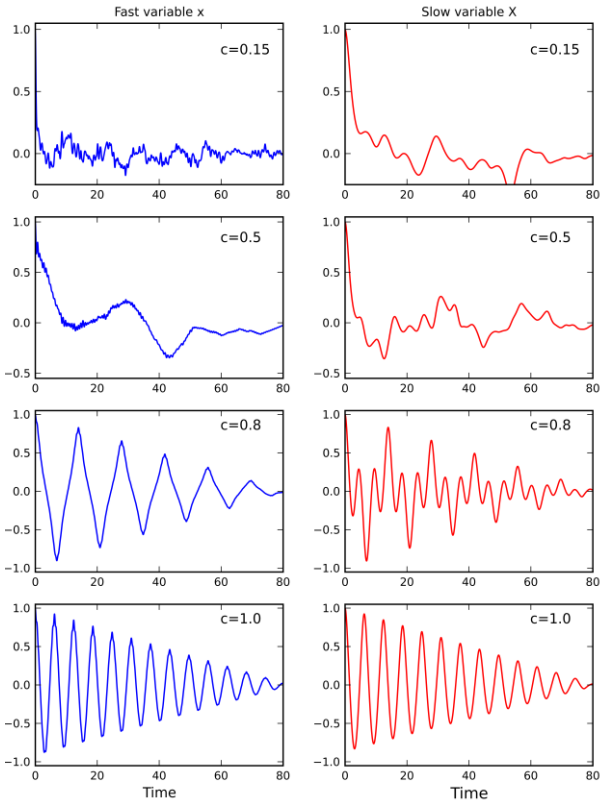

Fig. 3: Autocorrelation functions for dynamic variables *x* and *X* for different parameter *c*.

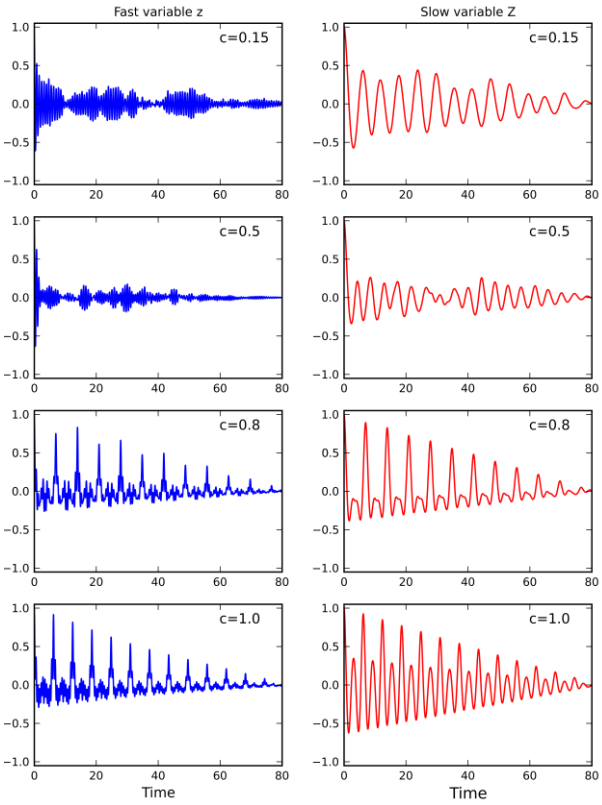

Fig. 4: Autocorrelation functions for dynamic variables *z* and *Z* for different parameter *c*.

However, as expected, the rate of decay of the ACF of the slow variable *X* is less than that of the fast variable *x*.

The ACFs for variables z and Z (really, their envelopes) also decay almost exponentially from the maximum to zero. For coupling strength parameter on the interval $0.4 < c < 0.6$ the ACF of the fast variable *x* becomes smooth and converges to zero. At the same time, the envelopes of the ACFs of variables *X*, *z* and *Z* demonstrate a fairly rapid fall, indicating the chaotic behaviour. As the parameter *c* increases, the ACFs become periodic and their envelopes decay slowly with time, indicating transition to regularity. For $c > 0.8$ calculated ACFs show periodic signal components.

3.5 Spectral properties

For a given discrete-time signal $\{u_m\}_{m=0}^{M-1}$ the power spectrum density (PSD) characterizes the signal intensity (power) per unit of bandwidth. For a wide-sense stationary process, the Wiener-Khinchin theorem relates the ACF to the PSD by means of a Fourier transform (i.e. PSD is a Fourier transform of ACF) and provides information about correlation structure of the time series generated by the system.

The term "power spectral density function" is frequently shortened to spectrum. The units of PSD are u^2/Hz, irrespective of what the units of *u* are. Oscillations of different types have specific spectral properties and, therefore, can be characterized by their PSD. For instance, a periodic motion consisting of the sum of finite number of sine curves has a set of lines in its spectrum, whereas a chaotic motion has a continuous spectral density function.

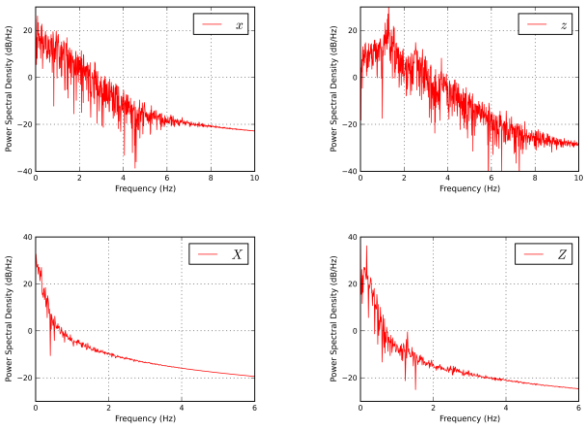

Fig. 5: PSD estimates of fast (*x* and *z*) and slow (*X* and *Z*) dynamic variables for *c*=0.15.

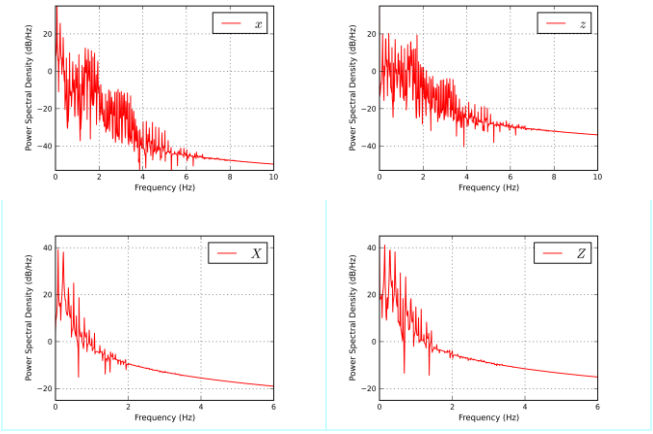

Fig. 6: PSD estimates of fast (x and z) and slow (X and Z) dynamic variables for c=0.8.

Generally, the ACF and spectrum represent different characterization of the same time series information. However, the ACF analyzes information in the time domain, and the spectrum in the frequency domain.

There are several methods, both parametric and nonparametric, for spectrum estimation [23, 24]. This paper uses periodogram, which is the most common nonparametric method for computing the PSD estimate of time series. This method calculates PSD based on the discrete Fourier transform (DFT). Let's define the DFT of sequence $\{u_m\}_{m=0}^{M-1}$ as

$$U_k = \sum_{m=0}^{M-1} u_m e^{-i(2\pi/M)mk}, \quad k = 0,\ldots,M-1,$$

where k is a discrete normalized frequency. Then the spectrum can be represented as follows

$$P_k = \frac{|U_k|^2}{Mf_s}, \quad k = 0,\ldots,M-1 .$$

The spectrum P_k can be plotted on a dB scale, relative to the reference amplitude P_{ref} =1, therefore

$$P_k^{dB} = 10 \cdot \log_{10}(P_k), \quad k = 0,\ldots,M-1.$$

The frequency f_k corresponding to point k of the DFT is

$$f_k = k\frac{f_s}{M}$$

The PSD estimates for fast (x and z) and slow (X and Z) variables as well as for weak (c=0.15) and strong (c=0.8) coupling are shown in Figs. 5 and 6, respectively. For weak coupling, the signal power for all dynamic variables decreases exponentially from low frequencies toward higher frequencies and distinctive energy peaks are not present for almost all variables. The only exception is the fast variable z, for which a local peak is observed at frequency ~1.2 Hz. For weak coupling, the spectrum of the fast subsystem is similar to the spectrum of the L63 model: the fast subsystem generates a broadband spectrum reminiscent of random noise corresponding to irregular aperiodic oscillations. At the same time, the low-frequency component strongly dominates in the spectrum of slow subsystem. As the coupling strength increases, the power spectrum of both fast and slow subsystems shifts toward the low frequencies, which predominate in the spectra.

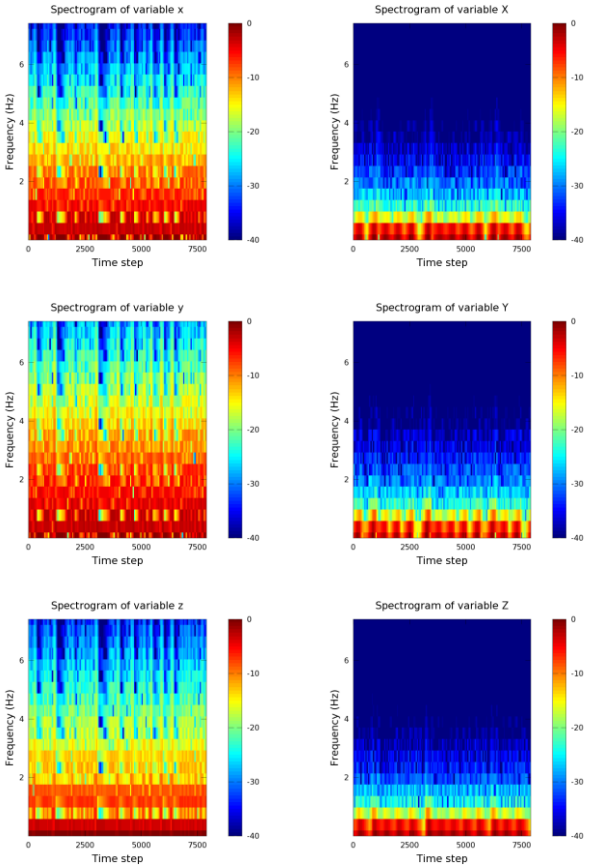

Fig. 7: Spectrogram for fast and slow dynamic variables for c=0.15.

Spectrogram is another powerful technique used in many applications for estimating the spectrum of the time series data. Spectrogram provides information about power as a function of frequency and time, and is generally presented as plot with the frequency of the signal shown on the vertical axis, time on the horizontal axis, and signal power on a colour-scale. Thus, for a given time frame the spectrogram provides the information about frequency content of a signal. Normalized

spectrograms for fast (x, y and z) and slow (X, Y and Z) variables for weak (c=0.15) and strong (c=0.8) coupling are shown in Figs. 7 and 8, respectively, with red color representing the highest signal power and blue the lowest. Calculated spectrograms are fully consistent with the PSPs, providing additional information about dominant and minor frequencies in the spectrum for a given time.

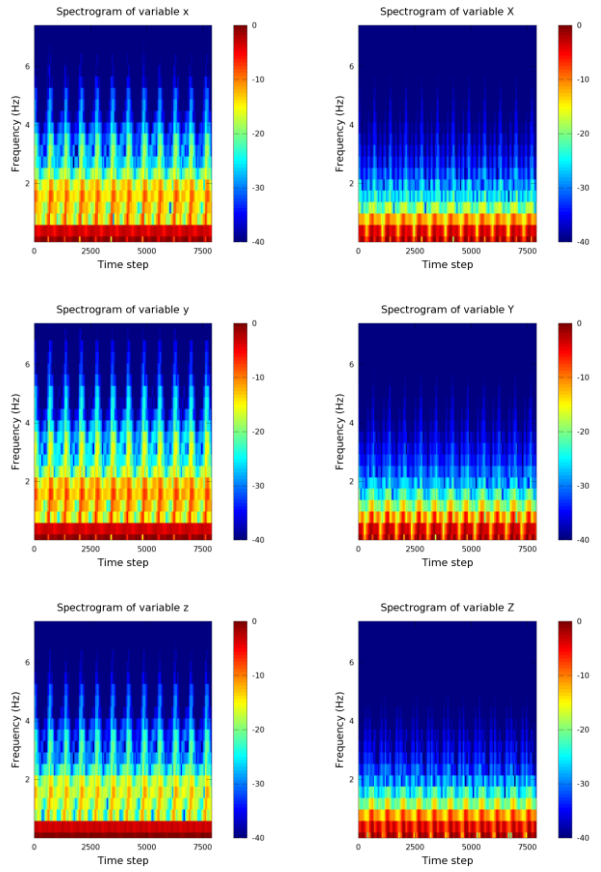

Fig. 8: Spectrogram for fast and slow dynamic variables for c=0.8.

4 Conclusion

The low-order coupled chaotic dynamical system discussed in this paper represents a powerful tool to study various physical and computational aspects of numerical weather prediction, data assimilation and climate simulation. However, the NWP and climate modeling pursue very different objectives and are focused on dynamical processes of significantly different spatial and time scales.

The integration time τ of the system equations can be classified based on its duration as short, intermediate, long and very long [14], with the corresponding values of τ set to τ = 0.1, τ = 0.44, τ = 2.26 and τ = 131.36, respectively. The short integration times traverse some portion of a trajectory along the attractor, the intermediate integrations correspond to complete circle around the attractor, the long integrations complete several circles, and the very long integrations correspond to movement along the attractor of about 100 times. The time step Δt=0.01 used in the numerical integrations is equivalent to 1.2 hours of a real time [7]. Therefore, intermediate and long-time intervals defined above correspond to 2.2 and 11.3 days, respectively, which are consistent with the NWP and data assimilation time of integrations. In turn, the very long integration intervals correspond to climate modeling time scales.

This paper analysed the basic dynamical, correlation and spectral properties of the nonlinear chaotic coupled dynamical system consisting of two versions of the L63 model. The autocorrelation functions, power spectrum densities and spectrograms for dynamic variables of the fast and slow subsystems were computed by numerical integration of the system equations. The influence of the coupling strength parameter on the ACFs, PSDs and spectrograms of system's dynamic variables was estimated.

By changing the coupling strength parameter c, one can obtain the system behaviour that reflects the major dynamical patterns of weather and climate for given natural conditions. The results of this paper can be applied to study multiscale chaotic dynamical processes occurring in complex technical systems, nature and society.

References:

[1] H.A. Dijkstra, *Nonlinear climate dynamics*, Cambridge University Press, New York, 2013.

[2] J. Marshall and R.A. Plumb, *Atmosphere, ocean and climate dynamics*, Academic Press, San Diego, 2007.

[3] J. Pedlosky, *Waves in the ocean and atmosphere*, Springer-Verlag, Berlin, 2nd edition, 2003.

[4] E. Kalnay, *Atmospheric modelling, data assimilation and predictability*, Cambridge University Press, Cambridge, 2003.

[5] T.T. Warner, *Numerical weather and climate prediction*, Cambridge University Press, Cambridge, 2011.

[6] F. Rabier, E. Klinker, P. Courtier, and A. Hollingsworth, Sensitivity of forecast to initial conditions, *Quarterly Journal of the Royal Meteorological Society*, Vol. 122, 1996, pp. 121-150.

[7] E.N. Lorenz, Deterministic non-periodic flow, *Journal of the Atmospheric Sciences*, Vol. 20,

1963, pp. 130-141.
[8] T.N. Palmer, Extended-range atmospheric prediction and the Lorenz model, *Bulletin of the American Meteorological Society*, Vol. 74, 1993, pp. 49-66.
[9] P.J. Roeber, Climate variability in a low-order coupled atmosphere-ocean model, *Tellus*, Vol. 47A, 1995, pp. 473-494.
[10] P. Gaurtier, Chaos and quadric-dimensional data assimilation: a study based on the Lorenz model, *Tellus*, Vol. 44 A, 1992, pp. 2-17.
[11] G. Evensen, Inverse methods and data assimilation in non-linear ocean models, *Physica D*, Vol. 77, 1994, pp. 108-129.
[12] R.N. Miller, M. Ghil, and F. Gauthiez, Advanced data assimilation in strongly non-linear dynamical systems, *Journal of the Atmospheric Sciences*, Vol. 51, 1994, pp. 1037-1056.
[13] L.A Smith, C. Ziehmann and K. Fraedrich, Uncertainty dynamics and predictability in chaotic systems, *Quarterly Journal of the Royal Meteorological Society*, Vol. 125, 1999, pp. 2855-2886.
[14] D.J. Lea, M.R. Allen, and T.W.N. Haine, Sensitivity analysis of the climate of a chaotic system, *Tellus*, Vol. 52A, 2000, pp. 523–532.
[15] J.D. Annan and J.C. Hargreaves, Efficient parameter estimation for a highly chaotic system, *Tellus*, Vol. 56 A, 2004, pp. 520-526.
[16] S. Soldatenko, D. Smith, P. Steinle and C. Tingwell, Sensitivity of coupled chaotic dynamical system to parameters in the context of data assimilation, *Journal of Mathematics and System Science*, Vol. 3, 2013, pp. 641-654.
[17] M. Peña and E. Kalnay, Separating fast and slow modes in coupled chaotic systems, *Nonlinear Processes in Geophysics*, Vol 11, 2004, pp. 319-327.
[18] L. Siquera and B. Kirtman, Predictability of a low-order interactive ensemble, *Nonlinear Processes in Geophysics*, Vol 19, 2012, pp. 273-282.
[19] C.Sparrow, *The Lorenz equations: bifurcations, chaos, and strange attractors*, Springer-Verlag, New York, 1982.
[20] F. Christiansen, G. Paladin, and H.H. Rugh, Determination of correlation spectra in chaotic systems, *Physical Review Letters*, Vol. 65, 1990, pp. 2087-2090.
[21] C. Liverani, Decay of correlations, *Annals of Mathematics*, Vol. 142, 1995, pp. 239-301.
[22] S. Panchev and T. Spassova, Simple general circulation and climate models with memory, *Advances in Atmospheric Sciences*, Vol. 22, 2005, pp. 765-769.
[23] A.V. Oppenheimer and R.W. Schafer, *Discrete-time signal processing*, Prentice Hall, 3rd edition, 2000.
[24] R.D. Hippenstiel, *Detection theory: Applications and digital signal processing*, CRC Press, Boca Raton, 2002.